

# Effect of Molecular Weight Distribution on Elongational Viscosity of Undiluted Polymer Fluids

B. H. BERSTED, *Research and Development Department, Amoco Chemicals Corporation, Amoco Research Center, Naperville, Illinois 60540*

## Synopsis

A combination of the Bersted model, giving the relaxation spectrum in terms of the molecular weight distribution (MWD), and the rubberlike-liquid model of Lodge is used to describe the elongational viscosity for constant extensional strain rates in terms of the MWD. Predictions of this hybrid model are in reasonable agreement with experimental results for polystyrene, if one assumes a strain rate dependent truncation of the relaxation spectrum. The predicted effects of varying molecular weight and breadth of the molecular weight distribution on the extensional viscosity are presented. At constant weight average molecular weight and constant strain, a narrower MWD is predicted to yield an extensional viscosity-strain rate curve that is essentially shifted to higher strain rates relative to a broader MWD. Furthermore, at constant weight, average molecular weight, constant strain, and high strain rates, a narrower MWD is predicted to yield a higher extensional viscosity.

## INTRODUCTION

In polymer processing operations molten polymer is often subjected to flow through short dies and variations of the spinning operation. In both of these cases the rheological response of the material is largely controlled by the elongational properties of the polymeric fluid, although the extensional strain rates cannot, in general, be considered constant in these processes.

There are two primary deformation modes, shear and elongational, studied for polymer melts. Simple shear has been studied extensively and its description in terms of molecular structure reported.<sup>1-6</sup> Conversely, elongational deformation is less well understood and studied. One of the major reasons for the lack of attention to elongational flow is the experimental difficulties in obtaining meaningful results. The lack of uniform and well-defined experimental conditions has led to apparently contradictory trends for the elongational viscosity with deformation rate.<sup>7</sup> However, more recently, increasing attention is being focused on the elongational behavior, since the flow behavior of polymeric melts in economically important processes such as fiber spinning, film blowing, and the extrusion through very short dies that are encountered commercially, is primarily governed by elongational rather than shear properties.

The elongational strain rate may be defined as  $\dot{\gamma}_E = dV_z/dz$ , where  $V_z$  is the velocity in the stretching direction  $z$ . If  $\dot{\gamma}_E$  is constant, the above relationship can be integrated to  $l/l_0 = e^{\dot{\gamma}_E t}$ , where  $l_0$  is the initial length. For the case of  $\dot{\gamma}_E$  not being constant, the situation increases greatly in complexity, and therefore will not be considered here. The elongational viscosity  $\eta_E$  may be defined as  $\sigma_E/\dot{\gamma}_E$ , where  $\sigma_E$  is the time-dependent tensile stress on the fiber (i.e., the load divided by the cross-sectional area). This case of constant strain rate is exper-

imentally realized for the uniform elongation of a rod, in which the one end is fixed and the other is separating from the fixed grip at constant velocity. This idealized case generally differs from the fiber spinning experiment in that  $\dot{\gamma}_E$  may not be constant and the cross-sectional area  $A$  of the fiber decreases along  $z$ .

In the past couple of years it has been demonstrated<sup>1-4</sup> that both the viscous and elastic properties of polymer melts are related in a simple manner to the molecular weight distribution (MWD). It is the intent of this paper to develop in a similar manner to the shearing case the relationship of elongational flow properties to the molecular weight distribution under conditions of constant rate of strain. This relationship will be developed by combining the previously developed connections between the relaxation spectrum and the molecular weight distribution and a simple, but more general, continuum model. The model chosen is the rubberlike-liquid model of Lodge.<sup>8</sup> This model has been chosen for the purpose of illustration and because of its simplicity.

## EXPERIMENTAL

The one sample studied here is an amorphous commercial polystyrene (Monsanto Company, Lustrex GC505) for which experimental elongational rheological behavior of this molten sample (155°C) at various constant extensional rates has been previously reported by Everage and Ballman.<sup>9,10</sup>

Molecular weight data were obtained with a Waters Model 200 GPC at 135°C using 1,2,4-trichlorobenzene as solvent and four Styrogel columns of porosities  $10^6$ ,  $10^5$ ,  $10^4$ , and  $10^3$  Å. Calibration was effected by using the universal calibration procedure with Pressure Chemical polystyrene standards.

## THEORY

The Bersted model,<sup>1-4</sup> relating rheological properties in shear to the MWD, makes no predictions for elongational flow. The model does, however, make the specific connection between the relaxation spectrum (from which most linear viscoelastic quantities may be calculated) and the MWD. Therefore, the model would appear to be able to provide the detailed molecular connection needed for making predictions from the MWD for arbitrary flows from the more general continuum models if these models can be described in terms of the relaxation spectrum. The Bersted model might be envisioned as serving a complimentary role to the more general theories, which lack detailed molecular connections.

The Bersted model assumes that linear viscoelastic relations are valid at higher shear rates, if the shear rate dependence of the system is taken into account. Therefore, the melt viscosity at any shear rate  $\dot{\gamma}$  can be represented as

$$\eta(\dot{\gamma}) = \int_0^{\tau_c} H(\tau) d\tau \quad (1)$$

where  $H(\tau)$  is the relaxation spectrum and  $\tau_c$  is a shear rate dependent parameter assumed to be proportional to  $1/\dot{\gamma}$ .  $\tau_c$  is therefore the maximum allowed relaxation time at any shear rate. The detailed connection between  $\eta(\dot{\gamma})$  and the molecular weight distribution has been made by using the empirical zero shear relationship to give the viscosity at  $\dot{\gamma}$  as

$$\eta(\dot{\gamma}) = K(\bar{M}_w^*)^a \quad (2)$$

where  $\eta_0 = K(\bar{M}_w)^a$  is the empirical zero shear relation,

$$\bar{M}_w^* = \sum_{i=1}^{i=c-1} w_i M_i + M_c(\dot{\gamma}) \sum_{i=c}^{\infty} w_i$$

and  $w_i$  is the weight fraction of the  $i$ th component.  $M_c(\dot{\gamma})$  was empirically found to be related to  $\dot{\gamma}$  as

$$M_c = M_0(\dot{\gamma})^d \quad (3)$$

where  $M_0$  is a constant depending on temperature and polymer type and  $d$  is a constant, which is approximately independent of temperature. It has recently been shown<sup>5,11</sup> that  $\tau_c$  can more accurately be represented as

$$\tau_c = \alpha(M_c)^a \quad (4)$$

where  $\alpha$  is a constant at a given temperature and for a given polymer type and  $a$  is the exponent in the zero shear relationship. It therefore follows that  $\tau_c$  is not necessarily proportional to  $1/\dot{\gamma}$  as assumed in earlier publications.<sup>1-4</sup>

The Bersted model has been extended to yield the relaxation spectrum in terms of the molecular weight distribution as

$$H(\tau_c) = \frac{K(\bar{M}_w^*)^{a-1} \bar{A}_2}{\alpha(M_c)^{a-1}} \quad (5)$$

where  $\bar{A}_2 = \sum_{i=c}^{\infty} w_i$  and  $\alpha$  is the proportionality constant between  $\tau_c$  and  $(M_c)^a$ .

A compatible general model to couple with the Bersted model is the rubberlike-liquid model of Lodge,<sup>8</sup> since the Lodge model appears to describe many of the rheological features of melts, if the relaxation spectrum is known. The Lodge model is given in terms of a memory function. In the Appendix, his model is redefined in terms of the relaxation spectrum, which using the Bersted model can be calculated from the MWD. Further, the time-dependent relaxation spectrum, which has previously been shown<sup>4</sup> to be applicable to time dependent shear properties, is used (see Appendix) to provide the following relationship for the extensional viscosity under conditions of constant rate of strain:

$$\begin{aligned} \eta_E = & \int_0^{\tau_c} \frac{H}{\tau} \left( \frac{2e^{2\dot{\gamma}_E t - t/\tau}}{2\dot{\gamma}_E - 1/\tau} + \frac{1}{\dot{\gamma}_E + 1/\tau} - \frac{2}{2\dot{\gamma}_E - 1/\tau} - \frac{e^{-(\dot{\gamma}_E t + t/\tau)}}{\dot{\gamma}_E + 1/\tau} \right) d\tau \\ & + \int_{\tau_c}^{\infty} \frac{H}{\tau} e^{-t/\tau_c} \left( \frac{2e^{2\dot{\gamma}_E t - t/\tau}}{2\dot{\gamma}_E - 1/\tau} + \frac{1}{\dot{\gamma}_E + 1/\tau} - \frac{2}{2\dot{\gamma}_E - 1/\tau} - \frac{e^{-(\dot{\gamma}_E t + t/\tau)}}{\dot{\gamma}_E + 1/\tau} \right) d\tau \end{aligned} \quad (6)$$

where  $H(\tau)$  is the relaxation spectrum at zero shear,  $\tau$  is the relaxation time,  $\dot{\gamma}_E$  is the steady elongational strain rate, and  $\tau_c$  is the maximum allowed relaxation time at long times (e.g., the relaxation time at which the spectrum is truncated). There is, however, no *a priori* reason to expect  $\tau_c$  in extensional flow to obey the same relationship as in shear with respect to the deformation rate, if in fact the relaxation spectrum is progressively truncated with increasing  $\dot{\gamma}_E$ . Two possible generalizations of eq. (3) will be considered. Equation (3) might be generalized by assuming a similar relationship as in eq. (3), but replacing  $\dot{\gamma}$  with the second invariant ( $\text{II} = -\dot{\gamma}^2$  in shear and  $-3\dot{\gamma}_E^2$  for extensional flow) of the strain rate tensor. The second possible generalization of eq. (3) involves replacing  $\dot{\gamma}$  with the maximum velocity gradient for more arbitrary flows. This would entail the

replacement of  $\dot{\gamma}$  with  $\dot{\gamma}_E$  in eq. (3) for extensional flows. This change is not incompatible with the principles of continuum mechanics (the viscosity being at most a function of the invariants of strain rate tensor), if we consider that in elongation flow the third invariant, III, of the strain rate tensor, which for mathematical convenience is generally considered to be zero, is not zero. Replacing  $\dot{\gamma}$  with  $\phi$  for nonviscometric flow yields the following expression in terms of the strain rate invariants:

$$\phi = (-II)^{1/2} + [1 - (3)^{1/2}/(2)^{1/3}](III)^{1/3}$$

## RESULTS AND DISCUSSION

### Comparison of Predictions with Experimental Data

Published data on linear polymers undergoing elongational flow at constant extensional rate, in which the sample length varies exponentially with time, are not very prevalent. The data of Everage and Ballman<sup>9,10</sup> have been chosen to compare with predictions, because the model of Bersted has already been shown to be applicable to the shearing case, and their data were obtained under conditions of isothermal steady elongational flow. The necessary parameters for application of the model have been shown<sup>5</sup> to be calculable from knowledge of the temperature variation of the zero shear viscosity. From the shear viscosity data of Everage and Ballman,<sup>9</sup> previously reported<sup>5</sup> values for  $\alpha$ ,  $M_0$ , and  $d$  at 190°C, and the predicted<sup>5,7</sup> temperature dependence of these parameters,  $K$  (155°C) was found to be  $6.21 \times 10^{-13}$ ,  $\alpha$  (155°C) =  $1.07 \times 10^{-18}$ ,  $M_0 = 221,000$ , and  $d = -0.2602$ .

As pointed out earlier, there is no *a priori* reason to expect  $\tau_c$  to bear the same relationship to deformation rate in the case of elongational flow as in shearing flow. As a result it would seem prudent to examine the predictions where the effect of elongation produces no progressive truncation of the relaxation spectrum with  $\dot{\gamma}_E$ . Figure 1 contains the experimental data of Everage and Ballman<sup>9</sup> and predictions of the model based on eqs. (5) and (6), where the effect of elongational flow on the relaxation spectrum is neglected (i.e.,  $\tau_c \equiv \infty$  and the relaxation spectrum is not truncated). For high  $\dot{\gamma}_E$  the predictions show the essential features of the experimental data, although the upturn at longer times is predicted somewhat earlier than observed. This predicted early upturn has also been observed by Chang and Lodge,<sup>12</sup> whose predictions from Lodge's rubberlike-liquid model, in which the memory function was evaluated from other rheological data in shear flow, were compared with Meissner's<sup>13</sup> experimental data on low-density polyethylene. These discrepancies between the experimental and predicted elongational viscosities at the higher deformation rates suggest that some truncation of the relaxation spectrum may be responsible.

The apparent deviations between the experimental and predicted data in Figure 1 at the lower  $\dot{\gamma}_E$  are harder to rationalize. From the data of Meissner<sup>13</sup> it was shown that at the beginning of stress growth, the experimental elongational viscosities coincided with the curve for the time-dependent shear case  $3\dot{\eta}_0(t)$ . Since it has been shown<sup>4</sup> that the Bersted model can give a good description of the shear stress growth  $[\dot{\eta}(t, \dot{\gamma})]$ , closer agreement between experimental elongational viscosities at low  $\dot{\gamma}_E$  and  $3\dot{\eta}_0(t)$  is expected. Additionally, agreement at low  $\dot{\gamma}_E$  with the shear case might be expected because of the reasonable

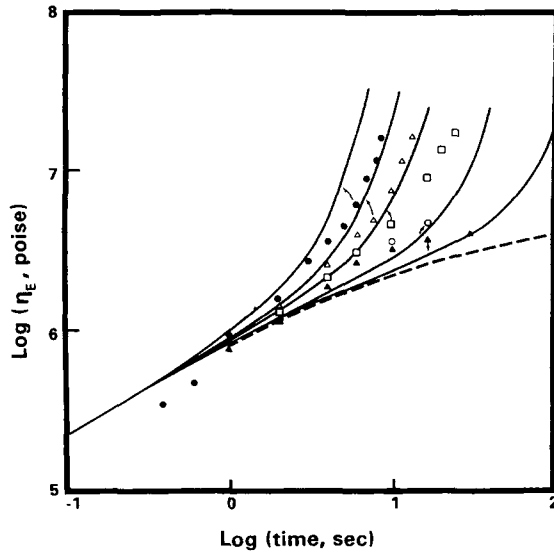


Fig. 1. Elongational viscosity as a function of strain rate and time. The lines are predictions of the model assuming no truncation of the relaxation spectrum, and the points are the experimental data of Everage and Ballman (ref. 9).  $\dot{\gamma}_E = (\bullet) 0.413, (\Delta) 0.260, (\square) 0.165, (\circ) 0.066, (\blacktriangle) 0.026 \text{ sec}^{-1}$ ; ---, predicted linear viscoelastic shear ( $3\dot{\eta}_0$ ).

agreement between predicted and experimental data reported by Chang and Lodge<sup>12</sup> at low  $\dot{\gamma}_E$ .

In order to attempt to improve agreement between the predictions and experimental data, the effect of deformation on the relaxation spectrum was assumed to be as given by eqs. (3) and (4), except  $\dot{\gamma}$  was replaced with the second invariant of the strain rate tensor. This modification led to much poorer agreement with experimental data; the upturn in the  $\eta_E$ -time curves was shifted to longer times than indicated by the experimental data at the higher strain rates, and poorer agreement at intermediate times was obtained at lower strain rates.

Another possible generalization of  $\tau_c$  to arbitrary flow situations involves the replacement of  $\dot{\gamma}$  with  $\dot{\gamma}_E$ , which as stated earlier implies that the third strain invariant of the strain rate tensor is not zero. The results are shown in Figure 2. As can be seen from Figure 2, better agreement with the experimental data is obtained at the highest  $\dot{\gamma}_E$  for the longer times than with the assumption of no truncation. No significant improvement at the lowest  $\dot{\gamma}_E$  is, however, evident.

The results in Figure 2 are replotted in Figure 3 such that the extensional viscosity is plotted versus elongational strain rate to give curves, which more closely resemble the flow curves obtained in the shear case. These plots resemble those obtained for the elongational component for converging flow through short dies as obtained by Shroff, Cancio, and Shida.<sup>14</sup> The resemblance may be a result of the approximately constant extensional strain a melt sees upon passage through a very short die, although the extensional rate is not constant. There is, however, some controversy<sup>14</sup> regarding the convergent flow analysis and its interpretation in terms of extensional flow.

While agreement between the predictions of the model from the MWD and

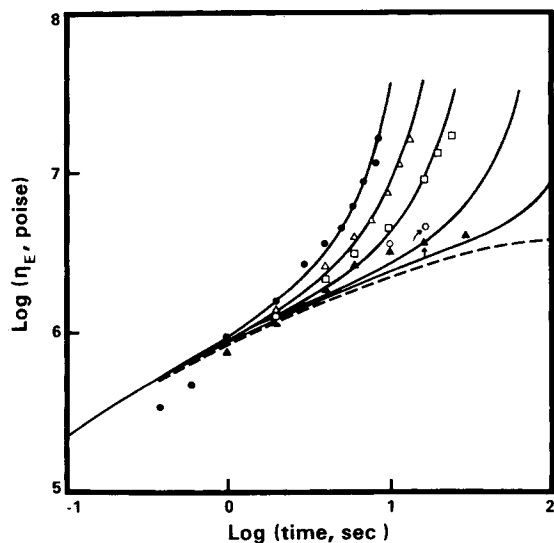


Fig. 2. Elongational viscosity as a function of time and strain rate. The predictions are made assuming the strain rate dependent truncation of the relaxation spectrum is similar in form to that found in shear—the strain rate in shear was simply replaced by the elongational strain rate. The values for  $\dot{\gamma}_E$  are the same as Figure 1.

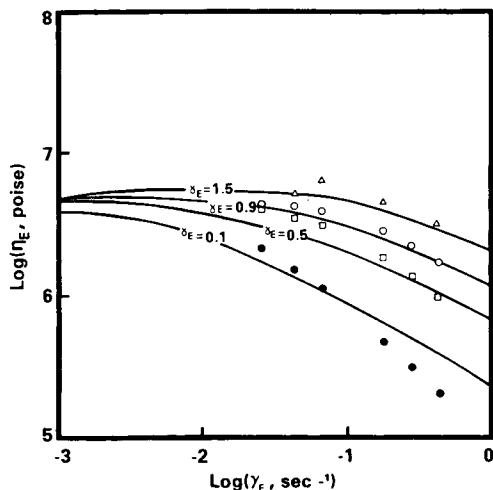


Fig. 3. Data in Figure 2 replotted such that the elongational viscosity is represented as a function of strain rate at constant strain levels (ref. 10).

the experimental data is not perfect, it should be pointed out that the predictions were made with no adjustable parameters, using only the constant  $K$  in the zero shear relation at  $155^\circ\text{C}$  and the constants  $\alpha$ ,  $M_0$ , and  $d$ , which had previously<sup>5</sup> been determined at  $190^\circ\text{C}$  for samples of completely different MWD's. Unlike the general continuum models,<sup>15,16</sup> whose parameters must be determined for each sample (generally from dynamic rheological data in shear) the present

model's parameters (determined for a given sample) can be used in making predictions for any other sample with an arbitrary MWD and with a similar molecular structure.

### Predicted Effects of Molecular Weight Distribution

The effects of varying the molecular weight distribution can be predicted using the model described here. These effects can be predicted from the MWD on an actual sample as obtained using GPC by varying the calibration curve. The breadth ( $\bar{M}_w/\bar{M}_n$ ) of the MWD was varied by changing the slope of the calibration curve for the GPC, but keeping  $\bar{M}_w$  constant. This had the effect of keeping the low shear viscosity and general "shape" of the MWD constant, but changing the breadth of the MWD. Conversely, the effect of the molecular weight at constant MWD breadth was effected by a GPC calibration curve shift with no calibration curve slope change.

The results of changing  $\bar{M}_w/\bar{M}_n$  at constant  $\bar{M}_w$  is shown in Figure 4, where  $\tau_c$  has been assumed to be a function of  $\dot{\gamma}_E = dV_z/dz$  from eqs. (3) and (4) by replacing  $\dot{\gamma}$  with  $\dot{\gamma}_E$ . From Figure 4 it is clear that the effect of increasing  $\bar{M}_w/\bar{M}_n$  is to broaden the maximum shown for high strains and to decrease  $\eta_E$  at high strain rates in a manner analogous to the case of steady shearing flow. Analogous to the shear case, the viscosities in Figure 4 appear to approach each other at constant strain for high strain rates. For the case of lower strains,  $\eta_E$  is lower for the broad MWD at all strain rates. The narrower MWD sample approaches more rapidly the Trouton viscosity (i.e.,  $3\eta_0$ ) at low  $\dot{\gamma}_E$  as might be expected for a narrower MWD sample having shorter terminal relaxation times. It should be pointed out that the maximum at high strains and the decreasing of  $\eta_E$  at high strain rates is not related to the assumption of the strain rate truncation of the relaxation spectrum; plots similar to Figure 4, in which no truncation of the re-

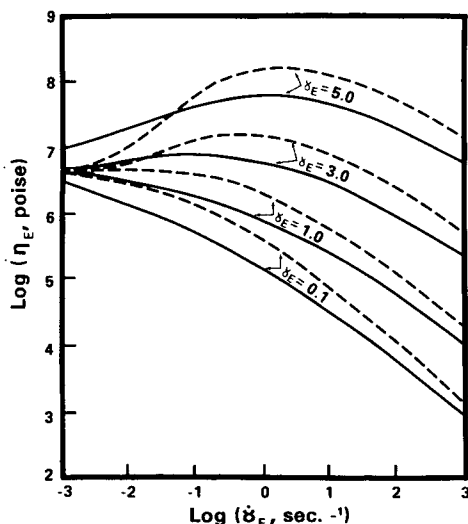


Fig. 4. Predicted effects of differing breadth of the molecular weight distribution on elongational viscosity at selected constant strain levels. The dashed line represents an MWD of  $\bar{M}_w/\bar{M}_n = 1.7$  and the solid line an MWD with  $\bar{M}_w/\bar{M}_n = 10.4$ . Both samples have  $\bar{M}_w = 245,000$ .

laxation spectrum was assumed in the calculations, produced all the characteristic features as in Figure 4.

These observations on the effect of MWD may be qualitatively rationalized as follows in terms of the spring-dashpot analogy (the generalized Maxwell model). The relaxation time  $\tau_i$  for a given relaxation mode is  $\eta_i/G_i$ , where  $\eta_i$  and  $G_i$  are the viscosity of the dashpot and the spring modulus, respectively. Now at constant  $\bar{M}_w$ , the effect of broadening the MWD is<sup>2</sup> such as to increase the largest relaxation times in the relaxation spectrum. These larger relaxation times are associated with increased  $\eta_i$  and compliances ( $1/G_i$ ). At low strain rates the deformation is dominated by the dashpots. In the limit where complete domination of the dashpots prevail,  $\eta_E = 3\eta_0$  (zero shear viscosity). If we consider that deviations from this relation are due to the rubberlike response of the springs, we would expect these deviations and behavior characteristics of rubberlike liquids to occur at lower strain rates for mechanisms associated with higher  $1/G_i$ , since it would take lower strain rates to produce spring elongation. Therefore we would expect deviations from the Trouton viscosity at lower extensional rates for the broader MWD as seen in Figure 4. At the very high strain rates mainly the spring will stretch with little dashpot movement. Since the spring stress is constant at a given strain and independent of  $\dot{\gamma}_E$ , the spring stress divided by  $\dot{\gamma}_E$  gives a decreasing  $\eta_E$  as a function of  $\dot{\gamma}_E$ . Since the broader MWD will have more compliant springs associated with its largest relaxation times, a lower stress is required at a given strain level and strain rate, with the result that at high strain rates a narrower MWD at constant  $\bar{M}_w$  leads to a higher apparent  $\eta_E$ . Therefore, we would expect that the extensional behavior of the broad MWD sample, having the largest relaxation times, to appear qualitatively shifted to lower strain rates.

Figure 5 shows the predicted elongational viscosity behavior for samples of equivalent MWD (identical  $\bar{M}_w/\bar{M}_n$  and  $\bar{M}_z/\bar{M}_w$ ) only differing in the absolute

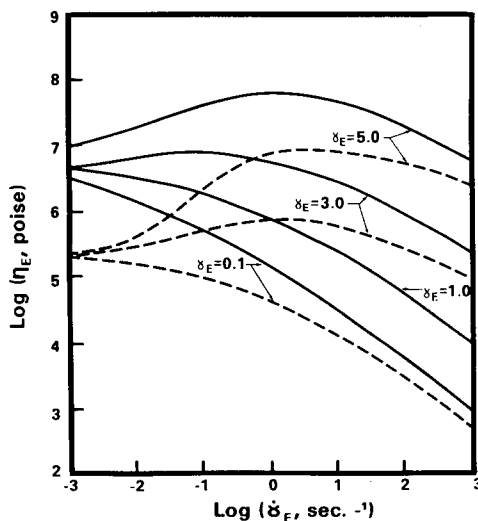


Fig. 5. Predicted effects of varying  $\bar{M}_w$  at constant  $\bar{M}_w/\bar{M}_n = 10.4$  on elongational viscosity. The dashed line represents a sample having  $\bar{M}_w = 101,000$  and the solid line a sample with  $\bar{M}_w = 245,000$ .



values of  $\bar{M}_n$ ,  $\bar{M}_w$ ,  $\bar{M}_z$ , etc. (i.e., one sample has a shifted molecular weight distribution). As can be seen from Figure 5, the elongational viscosity of the higher molecular weight sample is predicted to be higher at all strain rates at constant strain level. However, analogous to the case in Figure 4 and the shearing case,  $\eta_E$  for the samples of different molecular weight tend to approach each other at constant strain and at the high strain rates.

### Relevance to Fiber Spinning

The results and predictions dealt with here deal solely with isothermal elongational flow at constant strain rate, in which from the definition of constant extensional strain rate the velocity along a spinline must be a linear function of the spinline coordinate. In general, however, fiber spinning does not take place at constant strain rate, is not isothermal, and the stress (and therefore the elongational viscosity) varies along the spinline since the cross-sectional area of the extrudate varies along the spinline. Furthermore, the strain rates are orders of magnitude higher than those dealt with here. This last point does not present any problem in the making of predictions since the computer can easily calculate an elongational viscosity for these commercially interesting strain rates. A far more serious concern in attempting to apply the ideas expounded on here to spinning is the lack of constant strain rate. Even for isothermal spinning the whole history of a fluid element must be taken into account. Just what this history (diameter as a function of distance along the spinline) is in the spinning operation is not predictable from the MWD at this time. I am at present attempting to apply the predictions made here to the results obtained from Cogswell's<sup>14</sup> convergent flow analysis, for which the average history of a fluid element can presumably be predicted. Since the results of the convergent flow analysis have been shown<sup>14</sup> to be indicative of isothermal spinning results, it is hoped that valuable information on fiber spinning may be obtained from the application of the concepts explored here to Cogswell's convergent flow analysis.

Generally, in fiber spinning the thread breaks at some maximum stretch ratio ( $V_L/V_0$ , where  $V_L$  is the takeup velocity and  $V_0$  is the velocity of the melt in the spinnerette). If it is assumed that this maximum stretch ratio is associated with the strain softening<sup>17</sup> at higher values of the stretch ratio (which is related to the strain), a higher elongational viscosity would be expected to lead to a higher maximum stretch ratio. Calculations as in Figure 4 show that at constant  $\bar{M}_w$  and at the high strain rates in spinning operations a narrower MWD material has a higher elongational viscosity, which might be expected to allow the spinning to take place at higher takeup velocities until a threadline ductile failure takes place—in other words a narrower MWD is predicted to be more spinnable, in agreement with some reported experimental results.<sup>18</sup>

The above argument is no doubt a gross oversimplification since at least three (cohesive fracture, ductile, and "capillary") failure mechanisms have been identified<sup>19</sup> and found to be important in spinline failure. A more complete examination of this phenomenon in terms of predictions will be the subject of a future paper.

### Prediction of Elongational Viscosity from Steady Shearing Viscosity Data

It has been established that the steady shearing viscosity is predictable from the MWD. The results presented in this paper suggest that the elongational viscosity at constant strain rate is also predictable from the MWD. The question as to whether shear data is sufficient to predict the elongational viscosity has important implications, because of the inherent experimental difficulties in measuring the elongational viscosity.

In order to evaluate the elongational viscosity in terms of the rubberlike-liquid model of Lodge, the relaxation spectrum should be calculable. The relaxation spectrum has been shown to be calculable<sup>3</sup> from either the MWD or shear viscosity as a function of shear rate, once the functional relationship of the shear-dependent maximum-allowed relaxation time  $\tau_c$  is known.  $\tau_c$  has been evaluated for polystyrene<sup>5</sup> and high-density polyethylene<sup>2,5</sup> as a function of  $\dot{\gamma}$  to be

$$\tau_c = 1.67/(\dot{\gamma})^{0.885} \quad (7)$$

and

$$\tau_c = 2.13/\dot{\gamma}$$

respectively.

Consequently,<sup>2</sup> we get for HDPE,

$$H(\tau) = - \left[ \frac{(\dot{\gamma})^2}{2.13} \right] d\eta(\dot{\gamma})/d\dot{\gamma} \Big|_{\tau=2.13/\dot{\gamma}} \quad (8)$$

Finally, from eqs. (6) and (8), together with eq. (7), substituting  $\dot{\gamma}_E$  for  $\dot{\gamma}$ , the elongational viscosity can in principle be evaluated from steady shear viscosity data.

### CONCLUSIONS

The essential features of the rheological behavior of polymer melts undergoing isothermal elongational flow at constant strain rate can be adequately predicted from the molecular weight distribution by combining the rubberlike-liquid model of Lodge with the Bersted model. Comparison of predictions and experimental data at various constant extensional strain rates suggest that, in an analogous manner to shearing flow, the relaxation spectrum is progressively truncated with extensional rate. The functional relationship between the truncation and deformation rate appears to be the same for shear and elongation, suggesting that for nonviscometric flows the third strain rate invariant is not zero.

Both the experimental data of Ballman and Everage on polystyrene and predictions of the hybrid of the Lodge and Bersted models show that, depending on the strain rate and strain, the elongation viscosity can be constant, increase with strain rate, or decrease with strain rate.

The predicted effect of MWD is essentially as follows. At constant  $\bar{M}_w$  and strain the effect of narrowing the MWD on the elongational viscosity is to raise the viscosity at high strain rates and to appear to shift the extensional viscosity-strain rate curve to higher strain rates.

It is concluded that the elongational viscosity at constant strain rate could be

predicted from steady shear viscosity data, thereby eliminating the difficult task of making elongational viscosity measurements.

The author is indebted to Dr. A. Everage and Dr. R. Ballman for providing him with a sample of polystyrene, for which previously published experimental extensional data were available.

## APPENDIX: TIME DEPENDENT ELONGATIONAL VISCOSITY IN TERMS OF THE RELAXATION SPECTRUM

From Lodge's rubberlike-liquid model,<sup>8</sup> the elongational viscosity can be represented as

$$\eta_E = 1/\dot{\gamma}_E \int_{-\infty}^t \mu(t-t')(e^{2\dot{\gamma}_E(t-t')} - e^{-\dot{\gamma}_E(t-t')}) dt' \quad (1)$$

where  $\mu(t-t')$  is the "memory function,"  $t'$  is the past time, and  $t$  is the present time.

It has been shown by Janeschitz-Kriegl<sup>20</sup> that

$$\mu(t-t') = \frac{dG(t-t')}{dt'} \quad (2)$$

if  $G(t)$  vanishes at  $t = \infty$ . For suddenly imposed steady elongational flow at  $t' = 0$ , one has to use  $(t-t') = t$  for  $t' < 0$  and  $(t-t') = t-t'$  for  $t' \geq 0$ .

Substituting in eq. (1) for  $\mu dt$  from eq. (2), and using the above constraints, we get

$$\eta_E = \int_0^t G(\tau')(2e^{(2\dot{\gamma}_E\tau')} + e^{-(\dot{\gamma}_E\tau')}) d\tau' \quad (3)$$

where  $\tau' = t - t'$ .

Substituting the usual expression for the time-dependent shear modulus given in eq. (4) into eq. (3) and performing the

$$G(\tau') = \int_0^\infty \frac{H}{\tau} e^{-\tau'/\tau} d\tau \text{ and } \begin{cases} H(\tau, \dot{\gamma}_E, t) = H(\tau, 0) \text{ for } \tau \leq \tau_c \text{ (ref. 4)} \\ H(\tau, \dot{\gamma}_E, t) = H(\tau, 0) e^{-t/\tau_c} \text{ for } \tau > \tau_c \end{cases} \quad (4)$$

integration over  $\tau'$  yields

$$\eta_E = \int_0^{\tau_c} \frac{H}{\tau} \left( \frac{2e^{2\dot{\gamma}_E t - t/\tau}}{2\dot{\gamma}_E - 1/\tau} + \frac{1}{\dot{\gamma}_E + 1/\tau} - \frac{2}{2\dot{\gamma}_E - 1/\tau} - \frac{e^{-(\dot{\gamma}_E t + t/\tau)}}{\dot{\gamma}_E + 1/\tau} \right) d\tau \\ + \int_{\tau_c}^\infty \frac{H}{\tau} e^{-t/\tau_c} \left( \frac{2e^{(2\dot{\gamma}_E t - t/\tau)}}{2\dot{\gamma}_E - 1/\tau} + \frac{1}{\dot{\gamma}_E + 1/\tau} - \frac{2}{2\dot{\gamma}_E - 1/\tau} - \frac{e^{-(\dot{\gamma}_E t + t/\tau)}}{\dot{\gamma}_E + 1/\tau} \right) d\tau \quad (5)$$

## References

1. B. H. Bersted, *J. Appl. Polym. Sci.*, **19**, 2167 (1975).
2. B. H. Bersted, *J. Appl. Polym. Sci.*, **20**, 2705 (1976).
3. B. H. Bersted, *J. Appl. Polym. Sci.*, **21**, 2631 (1977).
4. B. H. Bersted, *J. Appl. Polym. Sci.*, **23**, 1279 (1979).
5. B. H. Bersted, *J. Appl. Polym. Sci.*, **23**, 1877 (1979).
6. W. W. Graessley, *Advances in Polymer Science Series*, Vol. 16, Springer-Verlag, New York, 1974.
7. C. D. Han, *Rheology in Polymer Processing*, Academic, New York, 1976.
8. A. Lodge, *Elastic Liquids*, Academic, New York, 1964.
9. A. Everage and R. Ballman, *J. Appl. Polym. Sci.*, **20**, 1137 (1976).
10. A. Everage and R. Ballman, *J. Appl. Polym. Sci.*, **21**, 841 (1977).
11. S. Pedersen and A. Ram, *Polym. Eng. Sci.*, **18**(13), 990 (1978).
12. H. Chang and A. Lodge, *Rheol. Acta*, **11**, 127 (1972).
13. J. Meissner, *Rheol. Acta*, **10**, 230 (1971).
14. R. Shroff, L. Cancio, and M. Shida, *Trans. Soc. Rheol.*, **21**(3), 429 (1977).
15. D. C. Bogue, *Ind. Eng. Chem. Fundam.*, **5**, 253 (1966).
16. A. S. Lodge, *Trans. Faraday Soc.*, **52**, 120 (1956).
17. N. Nitschmann and J. Schrade, *Helv. Chim. Acta*, **31**, 297 (1948).
18. C. D. Han, *Rheology in Polymer Processing*, Academic, New York, 1976, p. 208.

19. J. L. White, *Rubber Chem. Technol.*, **42**, 257 (1969).
20. H. Janeschitz-Kriegl, H. M. Laun, B. deCindio, M. Hansen, and F. Gortemaker, *Rheol. Acta*, **15**, 256 (1976).

Received October 2, 1978

Revised February 5, 1979